Astrophysical applications of quasar microlensing

E. Mediavilla[1], J. Jiménez-Vicente[2], and J.A. Muñoz[3]

[1] Instituto de Astrofísica de Canarias, Vía Láctea S/N, La Laguna 38200, Tenerife, Spain
[2] Departamento de Física Teórica y del Cosmos, Universidad de Granada, Campus de Fuentenueva, 18071 Granada, Spain
[3] Departamento de Astronomía y Astrofísica, Universidad de Valencia, 46100 Burjassot, Valencia, Spain

Abstract

We present a quick overview of several examples that illustrate the application of quasar microlensing to various problems of great interest in Astrophysics and Cosmology. We start introducing the main tool for simulating quasar microlensing, the magnification map. Then, the flux magnification statistics obtained from the magnification maps is used to study the quasar accretion disk size and temperature profile with results that challenge the thin disk model. The microlensing flux magnification statistics is also useful to determine the radial slope of the dark matter distribution in lens galaxies. The extremely high microlensing magnification at caustics allows to scan with horizon scale accuracy the quasar accretion disk, spiraling around the central super massive black hole, resolving the innermost stable circular orbit. Finally, transverse peculiar velocities of the lens galaxies, of great interest in cosmology, can be inferred either counting peaks in the microlensing light curves or directly from astrometric measurements of the highly magnified relative motions between lensed quasar images.

1   Introduction. Magnification maps.

When an intervening galaxy (the lens) gravitationally deflects the light from a distant quasar, several (typically two or four) observable images of the quasar can be formed. Each one of these images can, in turn, be split in microimages by the granulation in stars of the matter distribution of the lens galaxy. Microimages can not be resolved by telescopes but when the quasar moves with respect to the distribution of stars in the lens galaxy, the number and brightness of the microimages changes producing a change also in the total flux of the image (quasar microlensing; [2] and [19]).
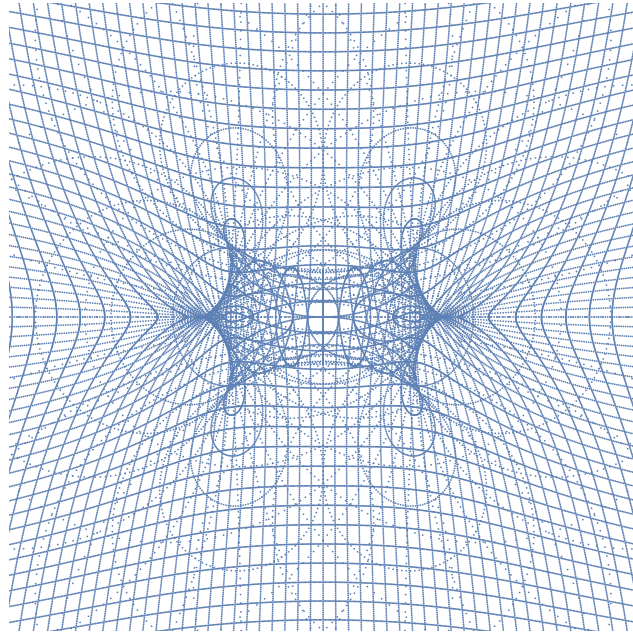
Figure 1: Inverse mapping of a regular lattice at the image plane onto the source plane. Each one of the deformed cells corresponds to a regular squared cell at the image plane. The magnification of a cell is, then, proportional to its area so that the smaller the cell the larger the magnification.

The primary observable of microlensing is, then, flux magnification, but as far as lensing is achromatic, according to Liouville's theorem, $I_\nu/\nu^3 = Cst.$, the intensity is going to be invariant and the flux of any of the images of the lensed quasar is going to be proportional to the surface subtended by the image, $dF = I_\nu d\Omega \propto d\Omega$. Then, to understand the effect of lensing we should understand the transformation of space induced by gravitational deflection. To do that we have inversely mapped the image plane, represented by a regular lattice, onto the source plane (see Fig. 1). The lens that we have used is the simplest non-trivial case, the binary lens, formed by two point objects, a binary star for instance. The result is very surprising. In the outer regions we see that the space is regularly deformed but in the central region we can identify a very well defined structure with several folds and cusps. This is a caustic curve. Magnification is large close to the caustic and formally infinity at the caustic. This is called a magnification map because it informs us about the way in which the lens magnifies space and, consequently, flux. When we consider that the light is deflected by a random distribution of stars (microlenses), we obtain magnification maps like the one in Figure 2 where many caustics of irregular shapes with cusps and folds are present. Magnification maps are the basic tool to simulate microlensing. Recent developments proposed to optimize their calculation [8, 7, 17, 18] allow to study with very high spatial resolution large regions of galaxies with a big number of microlenses.

The paper is organized as follows. In first place, we review the use of flux magnification statistics, inferred from magnification maps, to study the structure of the quasars accretion
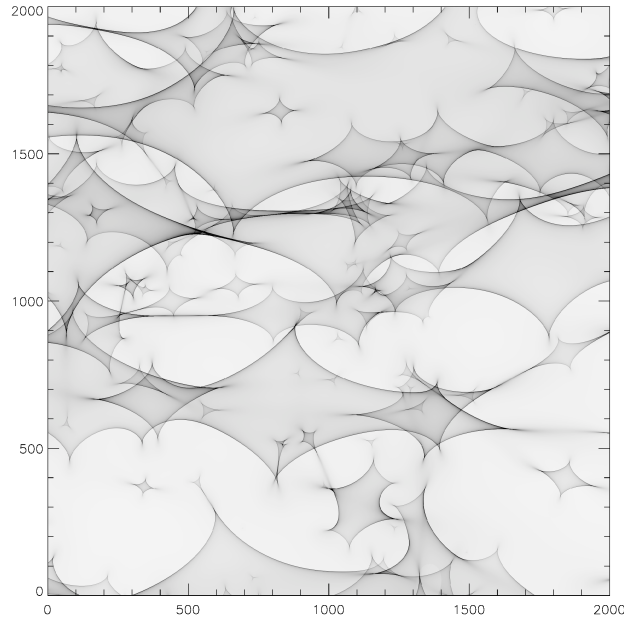
Figure 2:   Magnification map corresponding to a random distribution of stars in the lens galaxy.

disks (§2) and the dark matter profile of lens galaxies (§3). In §4 we describe how the high magnification at caustics can be used to dissect the innermost region of accretion disks. Finally, the statistics of caustic crossings can allow to determine the peculiar velocities of lens galaxies (§5.1), which may be also directly measured using the space magnification induced by lensing (§5.2).

2   Quasar accretion disk size and temperature profile

The probability of observing microlensing magnification of a given amplitude depends on the abundance of stars, i.e., on the fraction of the total mass in stars, α, in the lens galaxy. Microlensing is also sensitive to the size, r_s, of the unresolved quasar source (the putative accretion disk) so that the smaller the size the larger the microlensing magnification. According to this, it is usual to use a Bayesian approach to estimate these two parameters (α, r_s) from single-epoch microlensing measurements of a sample of lens systems (see, e.g. [13, 9, 12, 14, 5, 6]). The first step to do that is to compute magnification maps, for different values of α and r_s. From these maps the probability of measuring some magnification of the brightness of an image induced by microlensing, Δm_{micro}, given the parameters is obtained, $p(\Delta m_{micro}|\alpha, r_s)$. Then, using Bayes theorem, a probability is asigned to the interesting physical parameters (α, r_s), conditioned to the observed microlensing magnification, $p(\alpha, r_s|\Delta m_{micro}) \propto p(\Delta m_{micro}|\alpha, r_s)$.

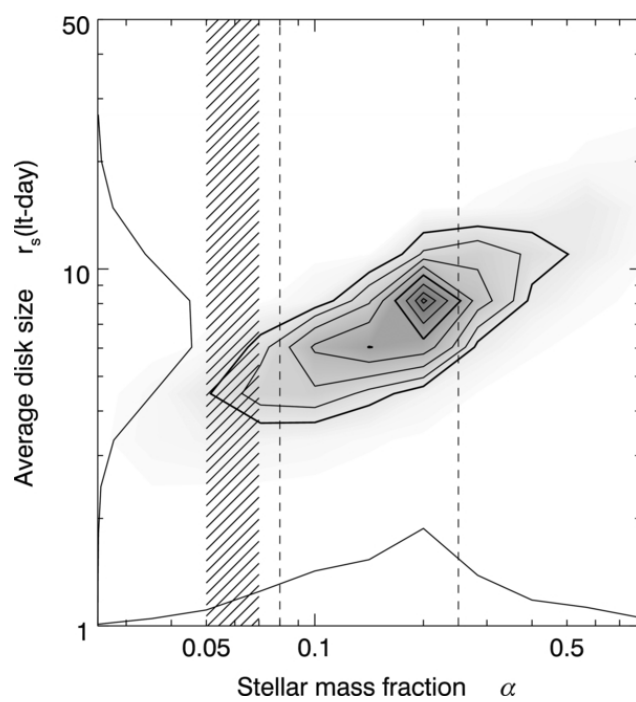In Fig. 3 we can see the probability density function obtained from 18 gravitational lens

Figure 3: 2D probability density function, $p(\alpha, r_s | \Delta m_{micro})$, of the fraction of mass in stars, α, and of the accretion disk size, r_s, inferred from the observed microlensing magnifications of 18 gravitationally lensed quasars, Δm_{micro}.
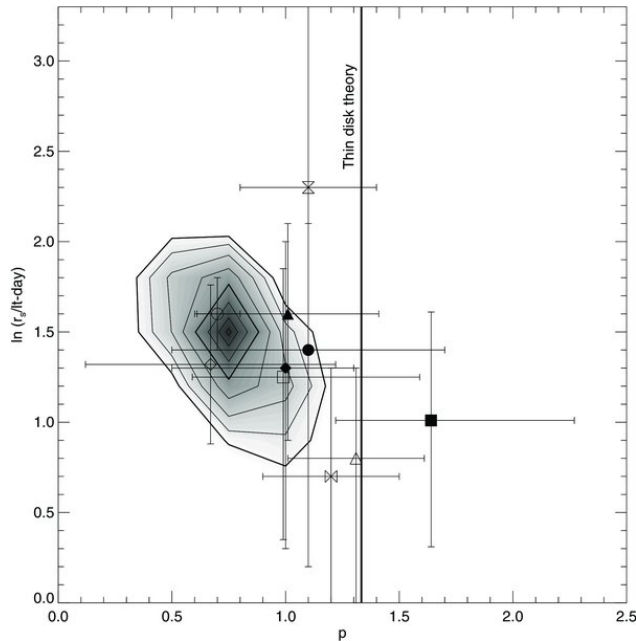
Figure 4:   2D probability density function, $p(p, r_s | \Delta m_{micro})$, of the logarithmic power-law slope defining the dependence of size with wavelength, p, $(r_s \propto \lambda^p)$, and of the accretion disk size, r_s, inferred from the observed microlensing magnifications at several wavelengths of 8 gravitationally lensed quasars, Δm_{micro}.

systems with measured microlensing magnification [5]. The joint probability, $p(\alpha, r_s | \Delta m_{micro})$, shows a clear covariance, in the sense of compensating a larger size with a larger abundance of microlenses (stars). However at 1σ the degeneracy is broken and we have rather well constrained results around the maximum of the probability distribution. The estimate of the fraction of mass in stars is relatively high with respect to previous results that did not take into account the covariance with the size and the estimate for the size is substantially greater than the predictions of the thin disk model [16].

Another important property of the accretion disk is the dependence of size with wavelength. Adopting a power law for this dependence, $r_s \propto \lambda^p$, and stacking the results for 8 gravitational lenses (Fig. 4), it is found (see [4] and references therein) that the observed chromaticity of size (dependence of size with wavelength) is significantly smaller than the predictions of the thin disk theory [16], in other words, that the temperature profile is steeper than expected.

3   Dark matter mass profile of lens galaxies

The previous results are based in the drastic assumption that all the images were at the same distance of the lens. To refine this approach, Jiménez-Vicente et al. [6] (see also [12]) have considered two samples of lensed images, grouping them according to their distance to
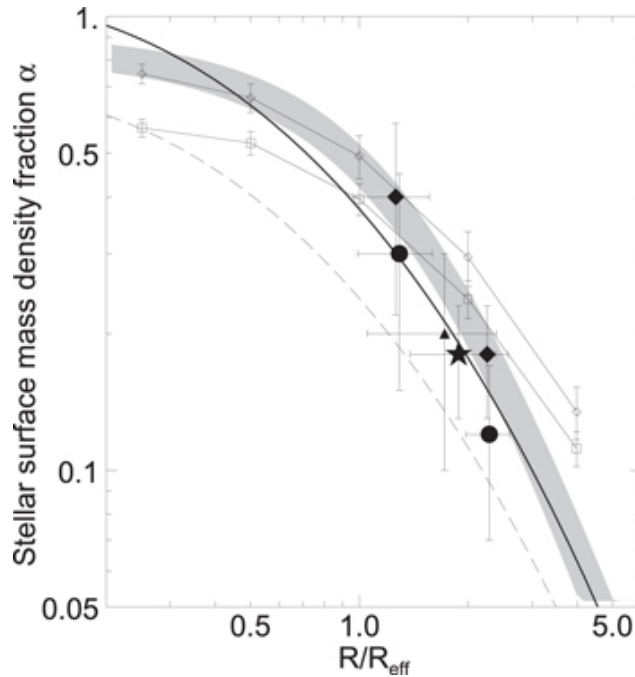
Figure 5: Stellar surface mass density fraction, α, versus distance in effective radius units. Diamonds (circles) correspond to linear (log) priors. Curves are scaled fiducial models.

the lens center. In spite of the large uncertainties, these authors have been able to obtain reasonable results considering two subsets of images corresponding to 18 gravitational lens systems. In Figure 5 we can see the two points of the radial profile obtained for either a linear or logarithmic prior [6]. The other curves in the plot represent some theoretical and semi-empirical models which in general show a good agreement in slope. It should be remarked here that, at difference with these curves, microlensing estimates are direct measurements, not based in strong modeling.

4   Scanning the innermost region of quasar accretion disks

Caustics can be used to scan the accretion disk. When, due to the relative movement between the source and the stars in the lens galaxy, an accretion disk crosses a caustic the disk luminosity profile is convolved with the caustic magnification profile (that rises like a delta function and then falls following a $\sqrt{D}$ dependence with the distance, D, to the crossing, see [15]). When the caustic crossing is clean (involves only a caustic), the resulting convolution, that is the resulting high magnification event in the light curve of the lensed image, can keep a great deal of information about the structure of the source.

In Figure 6 we can see the average of 3 clean caustic crossings corresponding to the quasar source in Q 2237+0305 (the Einstein Cross). In this Figure we can see that the thin disk [16] model (discontinuous line) cannot fit the fine structure present in the core of the
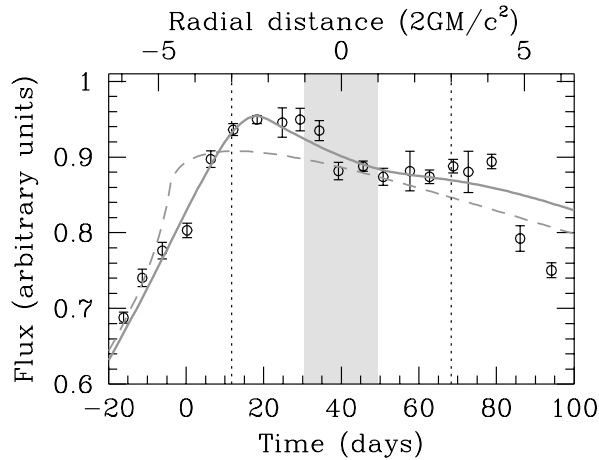
Figure 6: Caustic crossing fitting. Points correspond to the average of three high microlensing magnification events (likely clean caustic crossings) detected in the light curves of Q 2237+0305. The dashed (continuous) curve corresponds to non-relativistic (Schwarzschild including beaming) model of caustic crossing by an accretion disk. The grey region corresponds to the region inside the horizon and the vertical dotted lines to the ISCO.

average light curve which shows a central dip. To obtain a good matching to the dip, a model with relativistic beaming in the Schwarzschild metric (see [1, 10]) needs to be considered (continuous curve in Fig. 6). According to this model, we can identify the horizon (grey region borders in Fig. 6) and the Innermost Stable Circular Orbit (ISCO, vertical dotted lines in Fig. 6). Thus, caustic crossings can resolve the structure of the quasar accretion disks with horizon scale resolution. The future LSST monitoring will allow this study in many cases at different redshift.

5   Peculiar velocities of lens galaxies

Transverse velocities of lens galaxies can constitute a good statistical sample of the motion of galaxies with respect to the smooth Hubble flow. This peculiar motion of galaxies is crucial to understand the dynamics of the universe. In particular, peculiar velocities may be used to distinguish between different dark energy models which predicts the same geometry for the universe. We are going to present two different methods to estimate the peculiar velocities of lens galaxies from gravitational lensing.

5.1   Photometric method

Microlensing flux variability is caused by the relative movement between the galaxy and the source. Then, it should be possible to estimate the velocity of the lens galaxy from microlensing light curves. The measure of the relative velocity between the lens galaxy and
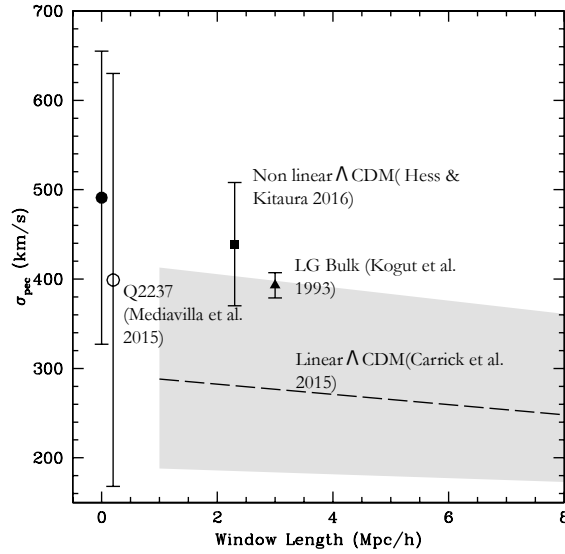
Figure 7: Peculiar velocity dispersion from several surveys and different characteristic scales. The filled circle corresponds to the peculiar velocity inferred from the counts of peaks in microlensing light curves of an ensemble of 17 lensed quasars. The dashed line is the prediction from linear ΛCDM.

the source can be easily understood if we consider that caustics are like randomly distributed milestones of known mean separation. Then the velocity will be proportional to the number of caustic crossings. One problem of this simple idea is that the crossing time is of about years and then, to control Poissonian noise we need to count caustic crossings, not in one, but in an ensemble of lens systems. Other problem is that if the source size is relatively large, the caustics are going to be smeared out. If we could use X-ray light curves, this would not be a problem, but there are only a few lenses monitored in X-Ray and we are forced to use optical light curves. In this case we need to consider the more general concept of counting Peaks Over a Threshold (POT).

To do a pilot study, Mediavilla et al. [11] have counted POT in an ensemble of 17 lensed quasars with light curves available in the literature obtaining direct estimates for the peculiar velocity dispersion at $z = 0.5$ of about $638 \, \mathrm{km \, s^{-1}}$ that can be scaled to $z = 0$, $\sigma(0) = 491 \, \mathrm{km \, s^{-1}}$. This last value (see Fig. 7) is compatible to within errors with ΛCDM predictions in the linear regime (the dashed line in Fig. 7), with the non-linear estimates by Hess and Kitaura [3], and with the estimate from the Local Group velocities.

In the next years, the number of available quasar microlensing light curves is going to increase by more than one order of magnitude with LSST and we expect to estimate with better accuracy peculiar velocities for different bins in redshift to test dark energy models.

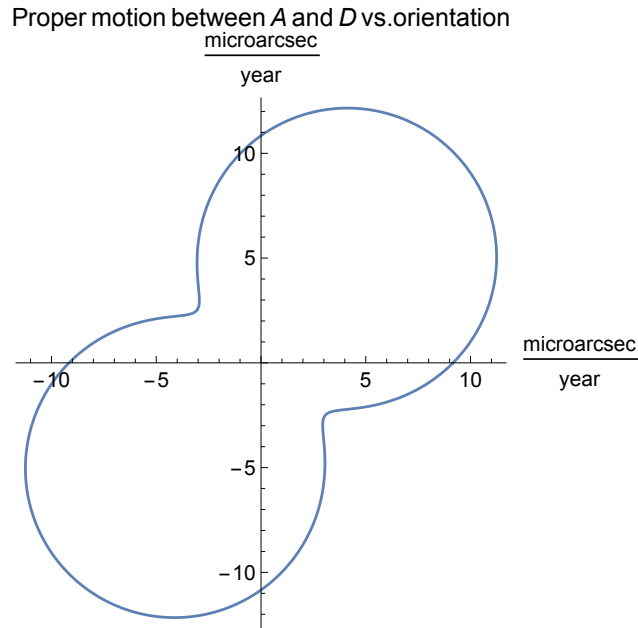Proper motion between *A* and *D* vs.orientation

Figure 8: Polar plot of the differential proper motion between images A and D of Q 2237+0305 (Einstein Cross). The distance to the origin corresponds to the length of the displacement after a year and the angle to the orientation of the galaxy motion.

5.2   Astrometric method

Counting peaks in the light curves is a way to estimate peculiar velocities but the most inmediate approach to estimate them is to measure directly the proper motion of the lens galaxy. But this is extremely difficult to do; a galaxy at $z = 0.3$ with a transverse velocity of $1000\,\mathrm{km\,s^{-1}}$, has an apparent motion of only 0.15 microarcsec per year.

However, lensing magnifies space and as a consequence, gravitational lenses magnify quasar apparent motion. Quantitatively, the proper motion between a pair of quasar lensed images depends on the orientation of the lens galaxy motion. For Q 2237+0305, the proper motion (see Fig. 8) can be of even 15 microarcsec per year. In 5 years it may be of about 75 microarcsec, something that may be within the limits of Gaia precision. Then it would be very interesting to analyze the first data release of Gaia to check its accuracy for differential astrometry between close sources. Other possibilities to obtain astrometry are VLBI, HARMONI at the E-ELT or even Theia (a proposed sucessor of Gaia with 20 times better astrometric accuracy).

6   Summary

We have performed a non-exhaustive tour around quasar microlensing phenomenology, presenting several results of general interest in Astrophysics and Cosmology. We can highlight

the following results:

1 - The size of the accretion disk spiraling around the central super massive black holes in AGN and quasars, is much greater than the predictions and its temperature profile is steeper than expected. Both results challenge the validity of the thin disk model and increase the difficulties to explain the observed quasar variability.

2 - The fraction of mass in compact objects (microlenses) in lens galaxies amounts 20% of the total mass in good agreement with the expectations for the stellar component (the slope of the radial gradient determined from microlensing is also in agreement with semi-empirical models that describe the stellar component) leaving no room for MACHOS or any type of compact object of non-stellar origin (Primordial Black Holes, for instance) in the extragalactic domain.

3 - Under favorable circumstances, caustic crossings can dissect the innermost regions of quasars with horizon scale resolution. Relativistic beaming at the internal rim of the accretion disc can explain the fine structure present in the caustic crossing events detected in Q 2237+0305. This is the first direct detection of structure, likely the ISCO, at $\sim$3 Schwarzschild radii in a quasar accretion disk. The monitoring of thousands of lensed quasars with future telescopes will allow the study of the horizon environments of black holes in hundreds of quasars in a wide range of redshifts ($0.5 < z < 5$).

4 - The transverse velocity field of lens galaxies (inferred from the statistics of microlensing peaks) can be a useful probe of cosmology through measurements of the linear growth rate that can distinguish between different dark energy models.

Acknowledgments

References

[1] Abolmasov, P., & Shakura, N. I. 2012, MNRAS, 423, 676

[2] Chang, K., & Refsdal, S. 1979, Nature, 282, 561

[3] Heß, S., & Kitaura, F.-S. 2016, MNRAS, 456, 4247

[4] Jiménez-Vicente, J., Mediavilla, E., Kochanek, C. S., et al. 2014, ApJ, 783, 47

[5] Jiménez-Vicente, J., Mediavilla, E., Kochanek, C. S., & Muñoz, J. A. 2015a, ApJ, 799, 149

[6] Jiménez-Vicente, J., Mediavilla, E., Kochanek, C. S., & Muñoz, J. A. 2015b, ApJ, 806, 251

[7] Mediavilla, E., Mediavilla, T., Muñoz, J. A., et al. 2011, ApJ, 741, 42

[8] Mediavilla, E., Muñoz, J. A., Lopez, P., et al. 2006, ApJ, 653, 942

[9] Mediavilla, E., Muñoz, J. A., Falco, E., et al. 2009, ApJ, 706, 1451

[10] Mediavilla, E., Jiménez-vicente, J., Muñoz, J. A., & Mediavilla, T. 2015, ApJL, 814, L26

[11] Mediavilla, E., Jimenez-Vicente, J., Munoz, J. A., & Battaner, E. 2016, arXiv:1609.02671

[12] Pooley, D., Rappaport, S., Blackburne, J. A., Schechter, P. L., & Wambsganss, J. 2012, ApJ, 744, 111

[13] Schechter, P. L., & Wambsganss, J. 2004, Dark Matter in Galaxies, 220, 103

[14] Schechter, P. L., Pooley, D., Blackburne, J. A., & Wambsganss, J. 2014, ApJ, 793, 96

[15] Schneider, P., & Weiss, A. 1987, A&A, 171, 49

[16] Shakura, N. I., & Sunyaev, R. A. 1973, A&A, 24, 337

[17] Vernardos, G., Fluke, C. J., Bate, N. F., Croton, D., & Vohl, D. 2015, ApJSS, 217, 23

[18] Vernardos, G., Fluke, C. J., Bate, N. F., & Croton, D. 2014, ApJSS, 211, 16

[19] Wambsganss, J. 2006, Saas-Fee Advanced Course 33: Gravitational Lensing: Strong, Weak and Micro, 453